Host–Guest Systems

DOI: 10.1002/ange.200601726

$(Ca_7N_4)[M_x]$ (M = Ag, Ga, In, Tl): Linear Metal Chains as Guests in a Subnitride Host**

*Peter Höhn, Gudrun Auffermann, Reiner Ramlau, Helge Rosner, Walter Schnelle, and Rüdiger Kniep**

A large number of ternary nitrides of the alkaline-earth metals (EA) with main-group or transition-metal elements contain "isolated" nitride ions, which are in an octahedral coordination environment and surrounded only by EA atoms. Condensation of the coordination polyhedra (EA_6N) through common corners and edges leads to structural patterns of various dimensionalities with different kinds of cavities,[1] which contain main-group and transition-metal species with various homo- or heteronuclear interconnections (e.g., $(Sr_6N)[Ga_5]$,[2] $(Sr_5N)[NbN_4]$,[3] $(Ca_3N)_2[FeN_3]$,[4] $(Ca_4N)[In_2]$,[5] $(Ca_3N)[Au]$[6]). Ternary nitrides with the composition $(Ca_7N_4)[M_x]$ (M = Ag, Ga, In, Tl) were first investigated in the late 1990s.[7,8] As essential details of the crystal structures remained unclear at that time, the data stayed unpublished. The main problems in understanding the chemical bonding in these compounds arose from the assumption that the (Ca_7N_4) partial structure should be positively charged (2+) and from the fact that the $[M_x]$ partial structure, an infinite linear chain, could not be clearly resolved (e.g., the value of x and the question as to whether there are additional N atoms within the chains). Meanwhile, we investigated the redox intercalation of binary EA subnitrides (EA_2N) and the formation of nitride diazenides.[9–11] The reactions are clearly controlled by EA species in a low-valence state (+1.5), which are structurally characterized by atomic positions associated with three condensed EA_6N octahedra ($EA_{6/3}N \triangleq EA_2N$). By taking into account this structural peculiarity of the low-valency EA species and by applying this principle to the $(Ca_7N_4)[M_x]$ series, we see that the Ca/N partial structure immediately appears as an uncharged mixed-valency subnitride ($Ca_3^{2+}Ca_4^{1.5+}N_4^{3-}$). The situation is depicted in Figure 1 and leads to the conclusion that there is no need for further charge balancing, which makes the central (linear) M_x chains an object of special interest.[12]

Single crystals of the highly hygroscopic phases, $(Ca_7N_4)[M_x]$, are obtained by treatment of Ca_3N_2 with M under N_2 or Ar at temperatures of approximately 1000 K.[13] The crystal structures of the orthorhombic phases (*Pbam*) were determined from X-ray data.[14] The (Ca_7N_4) framework consists of 2×2 chains of edge- and corner-sharing octahedra connected through common apices to form large channels running along [001]; M atoms are located inside the channels. A precise determination of the positional parameters for M from the diffraction data was virtually impossible.[14] As judged from electron-density calculations, the compositional indices, x, for the in-channel positions depend on the size of the M atoms and decrease with increasing size of the metal atom. The shapes and cross sections of the channels also depend on the M species incorporated, that is, increasing the size of the metal atom causes increasing "orthogonality". In contrast, the rigidity of the octahedral Ca/N building blocks (2×2 chains) is clarified by the almost constant c lattice parameter, which is independent of the in-channel M species. Relevant data that characterizes the crystal structures of the series $(Ca_7N_4)[M_x]$, M = Ag, Ga, In, and Tl, are included in Figure 1 and Figure 2 with the given parameter x derived from the crystal-structure refinements. The values of x should be taken as a first approximation and provide a first basis for comparison with the other experimental and theoretical results discussed below.

High-resolution electron microscopy (HREM) and electron diffraction (ED) were performed to obtain more information about the positions of the M atoms within the channels. Unfortunately, all representatives of the $(Ca_7N_4)[M_x]$ family readily hydrolyze when exposed to air, and only specimens of the silver compound, $(Ca_7N_4)[Ag_{1.36}]$, were amenable to ED experiments after preparation and transfer to the electron microscope under a strictly inert-gas atmosphere. High-quality HREM imaging was not possi-

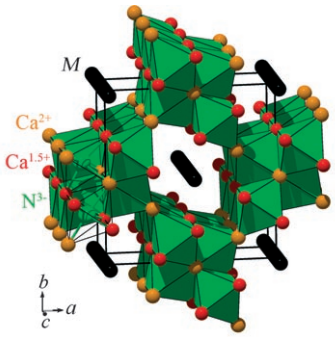

Pbam	Ag	Ga	In	Tl
Color	brass	bronze	bronze	brass
a [pm]	1145[a]	1147[b]	1168[b]	1158[b]
b [pm]	1203[a]	1208[b]	1213[b]	1200[b]
c [pm]	365[a]	364[b]	364[b]	363[b]
x	1.36	1.33	1.02	0.97
d(M-M) [pm]	269	274	356	373

[a] Neutron powder data.
[b] X-ray single crystal data.

Figure 1. Crystal structure of $(Ca_7N_4)[M_x]$. (Ca_7N_4) framework in polyhedral representation; the assignment of Ca^{2+} (orange) and $Ca^{1.5+}$ (red) ions is emphasized. $[M_x]$ is represented by black cylindrical rods inside the channels. Table: lattice parameters (space group *Pbam*) and occupancy x for $(Ca_7N_4)[M_x]$.[14]

[*] Dr. P. Höhn, Dr. G. Auffermann, Dr. R. Ramlau, Dr. H. Rosner, Dr. W. Schnelle, Prof. Dr. R. Kniep
Max-Planck-Institut für Chemische Physik fester Stoffe
Nöthnitzer Strasse 40, 01187 Dresden (Germany)
Fax: (+49) 351-46-46-3002
E-mail: kniep@cpfs.mpg.de

[**] We thank the Fonds der Chemischen Industrie for generous support, Ulrich Schwarz for fruitful discussions, Ulrike Schmidt and Anja Völzke for chemical analyses, Ralf Koban for physical properties measurements, and the BENSC (HMI Berlin) for access to their neutron facilities. H.R. thanks the Emmy Noether-Programm for financial support.

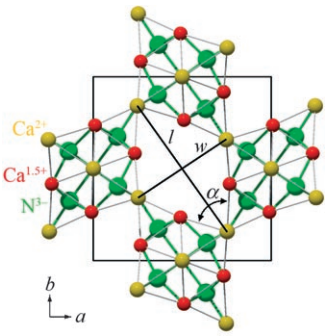

	$Ag_{1.36}$	$Ga_{1.33}$	$In_{1.02}$	$Tl_{0.97}$
l [pm]	1011	994	975	934
w [pm]	678	699	736	761
α [°]	67.7	70.2	74.1	78.3

Figure 2. Projection on the Ca/N partial structure along [001]. The shape of the channel is specified by the aperture angle α and the diagonals l and w of the rhombic cross section. Table: Values for l, w, and α are governed by the type of metal atom.

ble.[16] Selected-area electron diffraction (SAED) patterns of $(Ca_7N_4)[Ag_{1.36}]$ were registered for the [100], [110], and [010] zones (Figure 3). In all three zones, continuous diffuse lines can be discerned in addition to the Bragg reflections of the subnitride (and a product arising from hydrolyzation). Reconstruction in 3D reciprocal space results in sheets of diffuse intensity described by the plane equation $R = G \pm \varepsilon a^* \pm \eta b^* \pm \gamma c^*$, with ε, η being continuous variables and $\gamma = 1.357(25)$, which appear as first-order "satellites" to the subnitride Bragg-reflections $G = [hkl]^*$. Very weak second-order satellite sheets (lines) are also present. Such diffuse sheets are indicative of a 2D disordered (1D ordered) structure or substructure,[17] that is, perfectly periodic, identical, and parallel chains of atoms, which are not arranged regularly with respect to each other. Since two Laue conditions are violated, the scattering is concentrated on a family of parallel sheets (of first and higher order), which are normal to the chains of atoms and show a spacing that corresponds to the translational period along the chains. On the one hand, diffuse sheets of higher than first order are hardly visible. On the other hand, the pair of first-order sheets is multiplied by double (or multiple) diffraction, which is much more prevalent in ED than in X-ray or neutron diffraction.[18] As a result of double diffraction, a first-order pair of diffuse lines accompanies every systematic row of strong Bragg reflections, which extends horizontally, that is, orthogonally to c^* (Figure 3). In summary, the ED experiment shows that 1) the Ag atoms form chains with equidistant d(Ag–Ag) separations of 270(5) pm; 2) the chains are incommensurate with the subnitride structure; 3) there is no correlation between the z coordinates of Ag atoms (chains) in different channels, that is, the Ag chains are arbitrarily shifted along the channels.[17] Although it cannot be completely excluded that the chains might be interrupted by vacancies, thus leading to a loss of correlation even along a single channel, we favor the picture of the infinite chains with d(Ag–Ag) 270(5) pm, which gives $x = 1.36$, a value consistent with that derived from X-ray data ($x = 1.36$, d(Ag–Ag) 269 pm; Figure 1).[14] The incommensurate host–guest arrangement and the missing correlation between the Ag guest chains suggest quasi 1D behavior of these structural elements. Similar linear metal chains are observed in high-pressure modifications of the main-group elements K, Rb, Sr, Ba, As, Sb, and Bi,[19] and the transition metal, Sc.[20] The pairing of atoms within the 1D substructures, which is predicted to result from a Peierls distortion, is still under debate. To investigate the hypothesis of weakly interacting chains in a rigid host framework, electronic-structure calculations by using a full-potential local-orbital (FPLO) code were carried out.[21] To estimate the host–guest interaction, we calculated the band structure and the density of states (DOS) of a series of commensurate approximants. In all cases, only weak hybridization of the guest chains with the host lattice has been obtained. The band structure shows very pronounced 1D bands for the orbitals related to the guest chains, especially for the valence p_z orbitals. In the DOS, the corresponding van Hove singularities are present. Thus, the weak host–guest interaction estimated this way justifies the simulation of the guest chains by free, infinite, 1D chains. The in-chain bond length was optimized by using the total energy (Figure 4). The resulting value d(Ag–Ag) 266 pm is in good agreement with the bond lengths derived from SAED (270 pm) and from X-ray data (269 pm), thereby confirm-

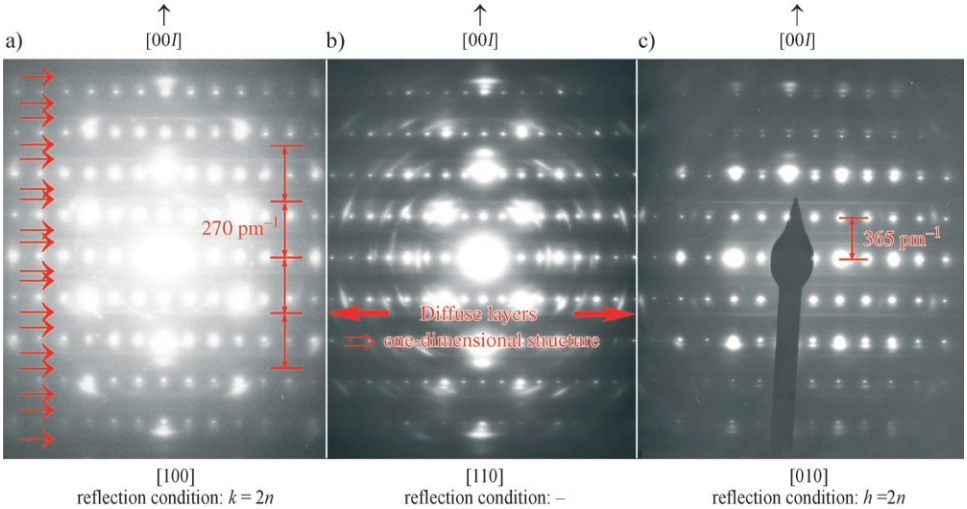

Figure 3. SAED patterns of $(Ca_7N_4)[Ag_x]$ in a) [100], b) [110], and c) [010] orientation taken from different microcrystals. All three patterns show continuous diffuse lines, which extend orthogonally to c^*. They appear as first-order "satellites" to the subnitride Bragg reflections at a distance $|q| = \gamma |c^*|$ with $\gamma = 1.357 \pm 0.025$. For further interpretation see text. The textured rings are attributed to some hydrolyzation product of the hypersensitive compound. The reason for the splitting of Bragg reflections is still unknown.

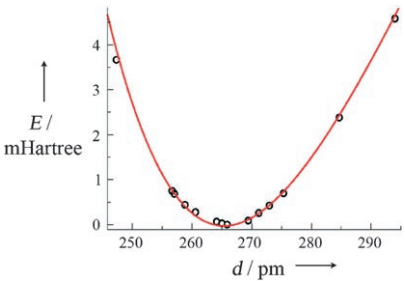

Figure 4. Energy versus bond length for an infinite, equidistant, and linear chain of Ag atoms. The red line is a fourth-order fit to the calculated data. The energy of the minimum at 266 pm is set to zero.

ing the picture of incommensurate metallic, 1D Ag guest chains in the (Ca_7N_4) subnitride host channels (Figure 5). The slightly smaller lattice parameter (about 1%) for the guest chain compared with the experimental data is a well-known systematic error arising from the local density approximation (LDA). We know from previous experience that the good agreement of the band-structure results with the guest chains and the experimental data is a strong indication of the excellent quality of the approximation of non-interacting guest chains in a rigid host. However, the metallic character of the resistivity (see below) for the Ag and the Ga compounds implies that the remaining interaction between the host and guest lattice is strong enough to inhibit a Peierls distortion, which would occur for a purely 1D chain and cause an insulating ground state. A detailed theoretical study of the host–guest interaction and its impact on the electronic structure will be undertaken.

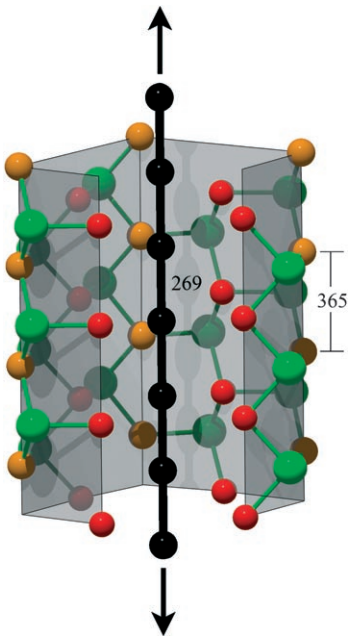

Figure 5. $[Ag_{1.36}]$ chain within a channel formed by the subnitride (Ca_7N_4). Front octahedra of the channel are omitted for clarity; Ca^{2+} orange, $Ca^{1.5+}$ red, and N green. Incommensurability is indicated by the given values for c (365 pm) and d(Ag–Ag) (269 pm, from X-ray data).

The optimization of the in-chain bonding distance d(M–M) by using the total energy, which is obtained by the same procedure as that presented in Figure 4, yields 278 pm (M = Ga), 305 pm (In), and 317 pm (Tl). Although the calculated value for the Ga chain is in good agreement with the distance derived from the X-ray investigation ($x = 1.33$, d(Ga–Ga) 274 pm), the calculated distances for In and Tl are much shorter than the respective values based on $x = 1.02$ (d(In–In) 356 pm) and $x = 0.97$ (d(Tl–Tl) 373 pm).[14]

For $(Ca_7N_4)[In_x]$, we were able to prepare a larger amount of single-phase material and a chemical analysis was carried out that gave $x = 1.06(1)$,[22] which is close to the X-ray value ($x = 1.02$) and is unequivocally smaller than the value obtained by calculations based on the assumption that the chains of In atoms are equidistant, $x = 1.19$. This lower value suggests the presence of In–In chain fragments within the host channels with average lengths consistent with the observed composition. The same model holds for the Tl compound. To date, there is no evidence for significant variations in the compositional index, x, for the In and Tl compounds, but this observation has to be investigated in more detail.

From a structural point of view, the $(Ca_7N_4)[M_x]$ family can be divided into two groups: the Ag and Ga compounds with infinite host chains of equidistant metal atoms, and the In and Tl phases, which contain metal-chain fragments. For infinite chains, metallic conductivity can be expected, whereas segments of metallic chains would exhibit activated electronic conduction.

The electrical resistivities, $\rho(T)$, of cold-pressed powder samples of the four compounds were investigated by using the van der auw method (Figure 6). The Ag compound clearly

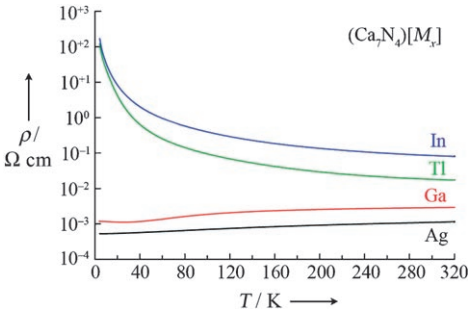

Figure 6. Electrical resistivity, ρ, versus temperature, T, for cold-pressed powder samples of $(Ca_7N_4)[M_x]$. The measurement was performed by the van der Pauw method in a die cell made of a sapphire crystal.

displays a linear temperature dependence with $\rho(T)$ increasing with T and a room-temperature resistivity around 1 mΩ cm, which indicates a metallic conductor, albeit a poor one. The resistivity of the Ga compound is metallic above about 30 K (increasing with temperature), but shows a weak upturn below this temperature. The In and Tl compounds exhibit a thermally activated conduction mechanism. Note in powder samples, the metallic regions of the crystallites are generally interrupted, thus increasing the overall resistivity. In the In and Tl compounds, the metal chains are assumed to be

interrupted on the atomic scale. Simple statistics suggest that with the given values of x and the calculated equilibrium distances of the M atoms, average chain lengths for M = In and Tl are 1824 and 1794 pm, respectively. A closer inspection of the temperature dependence of $1/\rho$ of these samples reveals that their conduction mechanism can be well described by 3D variable range hopping with an exponent $\gamma = 1/4$,[23] as could be expected for an ensemble of fragmented conducting, metallic chains. Only the Ag compound behaves like a metal powder a result that is compatible with uninterrupted infinite chains of M.

Powdered samples of $(Ca_7N_4)[M_x]$ (M = Ag, Ga, In, and Tl) show a paramagnetic susceptibility (Figure 7). The susceptibilities are interpreted as the sum of weakly temper-

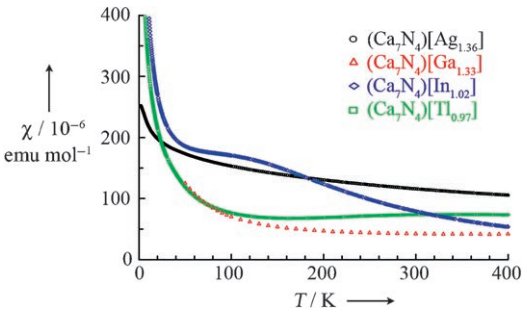

Figure 7. High-field magnetic susceptibility $\chi = M/H$ (M magnetic moment, H magnetic field strength versus T. The data were measured in $\mu_0 H = 7$ T and were corrected for ferromagnetic impurities.

ature-dependent paramagnetic contributions and low-temperature upturns from Curie-like impurities. Thus, the materials are Pauli-paramagnetic metals with occupied states at the Fermi level, E_F, which confirms the metallic character of the chains or chain segments in all four compounds. The weakly temperature-dependent Pauli-paramagnetic contribution, χ_P, and the diamagnetic core contributions, χ_{dia}, can not be separated easily. However, we estimate $\chi_P \approx 300 \times 10^{-6}$ emu mol^{-1} for the Ag and In compounds. This value corresponds to a density of states, $N(E_F) =$ 9–10 states eV^{-1} f.u.$^{-1}$ (f.u. = formula unit). For the compounds with M = Ga, Tl, about half the density of states is estimated.

In conclusion, we have presented a series of compounds consisting of a mixed-valent subnitride host structure ($Ca_3^{2+}Ca_4^{1.5+}N_4^{3-}$) containing parallel channels that are incommensurably filled with linear chains of equidistant metal atoms (M = Ag, Ga) or fragments of linear chains of equidistant atoms (M = In, Tl) that interact only weakly with the host lattice. Experimental results and theoretical calculations carried out so far lead to a consistent picture, which will be the basis for future work. Our main focus is to grow and prepare single crystals suitable for the measurement of physical properties in the directions parallel and perpendicular to the metal chains. Further TEM investigations are needed, including HREM imaging, which is dependent on the purity and stability of the samples. The question of a possible homogeneity range for the In and Tl compounds has to be answered and there is a need for further experimental evidence concerning the valence states of the elements involved. Finally, we will investigate whether there are other metal atoms, besides Ag, Ga, In, and Tl, that fit within this type of subnitride structure—altogether a challenging program for the future.

Received: May 2, 2006
Revised: June 19, 2006
Published online: September 15, 2006

Keywords: ab initio calculations · host–guest systems · nitrides · subvalent compounds

[1] P. Höhn, R. Kniep, *Z. Anorg. Allg. Chem.* **2002**, *628*, 2174.
[2] G. Cordier, M. Ludwig, D. Stahl, P. C. Schmidt, R. Kniep, *Angew. Chem.* **1995**, *107*, 1879; *Angew. Chem. Int. Ed. Engl.* **1995**, *34*, 1761.
[3] P. Höhn, R. Kniep, *Z. Anorg. Allg. Chem.* **2002**, *628*, 463.
[4] G. Cordier, P. Höhn, R. Kniep, A. Rabenau, *Z. Anorg. Allg. Chem.* **1990**, *591*, 58.
[5] M. Kirchner, W. Schnelle, F. R. Wagner, R. Kniep, R. Niewa, *Z. Anorg. Allg. Chem.* **2005**, *631*, 1477.
[6] J. Jaeger, D Stahl, P. C. Schmidt, R. Kniep, *Angew. Chem.* **1993**, *105*, 738; *Angew. Chem. Int. Ed. Engl.* **1993**, *32*, 709.
[7] M. Ludwig, Dissertation, TU Darmstadt **1998**.
[8] J. Jäger, Dissertation, TU Darmstadt, **1995**.
[9] G. Auffermann, Y. Prots, R. Kniep, *Angew. Chem.* **2001**, *113*, 565; *Angew. Chem. Int. Ed.* **2001**, *40*, 547.
[10] G. V. Vajenine, G. Auffermann, Y. Prots, W. Schnelle, R. K. Kremer, A. Simon, R. Kniep, *Inorg. Chem.* **2001**, *40*, 4866.
[11] Y. Prots, G. Auffermann, M. Tovar, R. Kniep, *Angew. Chem.* **2002**, *114*, 2392; *Angew. Chem. Int. Ed.* **2002**, *41*, 2288.
[12] P. Höhn, R. Ramlau, H. Rosner, W. Schnelle, R. Kniep, *Z. Anorg. Allg. Chem.* **2004**, *630*, 1704.
[13] Single-phase powder samples of $(Ca_7N_4)[M_x]$ (M = Ag, Ga, In, and Tl) are synthesized by the reaction of appropriate mixtures of Ca_3N_2 [from calcium (Alfa, 99.98 %) loaded in a tungsten crucible in a stream of N_2 (Messer Griesheim, 99.999 %, purified with a Merck BTS catalyst) for 24 h at 1023 K] and the respective metals, M (Alfa, > 99.9 %) in tantalum crucibles at temperatures of 1123 K for 48 h under an Ar atmosphere (Messer Griesheim, 99.999 %, purified with a Merck BTS catalyst). Repeated reactions with intermediate regrinding and reforming of pellets were employed. Small amounts of needlelike single crystals were prepared by using a small excess of Ca in the reaction mixtures.
[14] For single crystal X-ray diffraction experiments, a STOE IPDS diffractometer was used: $(Ca_7N_4)[Ga_{1.33(1)}]$/(Ca_7N_4)-$[In_{1.02(1)}]$/$(Ca_7N_4)[Tl_{0.97(1)}]$; $Mo_{K\alpha}$, graphite monochromator, $T =$ 298 K; 1256/1220/1229 measured, 660/703/646 unique reflections; $R = 0.044/0.051/0.082$, $R_w = 0.104/0.121/0.218$. Neutron diffraction experiments were carried out on the powder diffractometer E9 at the reactor BER II of the HMI Berlin: (Ca_7N_4)-$[Ag_{1.36(2)}]$; w$R_{profile} = 0.0468$, $R_{Bragg} = 0.0723$, 415 observed reflections. The samples were sealed under argon into cylindrical vanadium containers (diameter 8 mm, length 47 mm, wall thickness 0.15 mm), which were closed with caps containing an indium seal. Crystal-structure data derived from neutron diffraction experiments with the wavelength $\lambda = 1.79704(2)$ Å in the range $2° \le \Theta \le 158°$. The refinements were carried out by using the program Fullprof.[15] Structure determination and crystallographic data: $(Ca_7N_4)[Ag_{1.36(2)}]$, $(Ca_7N_4)[Ga_{1.33(1)}]$, $(Ca_7N_4)[In_{1.02(1)}]$, $(Ca_7N_4)[Tl_{0.97(1)}]$; orthorhombic, *Pbam*; $a =$ 1144.8(1)/1147.4(1)/1168.1(2)/1158.3(1) pm, $b =$ 1202.9(1)/1208.0(1)/1212.9(2)/1199.6(1) pm, $c =$ 365.2(1)/363.6(1)/

364.3(1)/362.8(1) pm; $Z=2$, $\rho_{calc}=3.18/2.84/2.93/3.52\ g\,cm^{-3}$. The x values were determined by adding up the electron density within the channels under the assumption of exclusive occupation by metal. Further details on the crystal-structure investigation may be obtained from the Fachinformationszentrum Karlsruhe, 76344 Eggenstein-Leopoldshafen, Germany (fax: (+49) 7247-808-666; e-mail: crysdata@fiz-karlsruhe.de), on quoting the depository numbers CSD-416506, -416502, -416501, and -416500.

[15] J. Rodriguez-Carvajal, Laboratoire Léon Brillouin, Saclay FULLPROF. 2 K Version 3.40, November **2005**.

[16] The Tecnai G^2F30 electron microscope (spherical aberration constant $C_S=1.2$ mm) with field emission gun was operated at 300 kV. Selected-area electron-diffraction patterns were registered on photographic film and with a Gatan US-CCD camera (2048 × 2048 pixels). Microcrystallites appropriate for ED were prepared in a glove box (argon atmosphere) by finely crushing the polycrystalline compound. The hypersensitive specimens were mounted in standard holders and transferred to the microscope by using an inert gas shuttle system.

[17] a) A. Guinier, *X-ray diffraction in crystals, imperfect crystals, and amorphous bodies*, Dover Publications, **1994**; b) F. Frey, *Acta Crystallogr. Sect. B* **1995**, *51*, 592.

[18] R. L. Withers, *Z. Kristallogr.* **2005**, 220, 1027.

[19] a) U. Schwarz, *Z. Kristallogr.* **2004**, *219*, 376; b) M. McMahon, R. J. Nelmes, *Z. Kristallogr.* **2004**, *219*, 742; and references therein.

[20] a) H. Fujihisa, Y. Akahama, H. Kawamura, Y. Gotoh, H. Yamawaki, M. Sakashita, S. Takeya, K. Honda, *Phys. Rev. B* **2005**, *72*, 132103; b) M. I. McMahon, L. F. Lundegaard, C. Hejny, S. Falconi, R. J. Nelmes, *Phys. Rev. B* **2006**, 73, 134102.

[21] K. Koepernik, H. Eschrig, *Phys. Rev. B* **1999**, *59*, 1743. In the scalar-relativistic calculations, the exchange and correlation potential of Perdew and Wang (J. P. Perdew, Y. Wang, *Phys. Rev. B* **1992** *45*, 13244) was used. As the basis sets, Ga (3s, 3p, 3d, 4s, 4p), Ag and In (4s, 4p, 4d, 5s, 5p), and Tl (5s, 5p, 5d, 6s, 6p) states were employed. The lower lying states were treated fully relativistically as core states. A k mesh of 1056 points (30 intervals along the chain direction) in the irreducible part of the Brillouin zone (12000 in the full zone) was used to ensure accurate total energies, density of states and band-structure information.

[22] The metallic components were analyzed with an inductively coupled plasma optical emission spectrometer (ICP–OES; Varian Vista RL). The nonmetallic components, N, O, H, and C, were quantitatively determined by the carrier-gas hot-extraction or combustion technique (LECO TC 436 DR/5, RH 404, and C200CHLH): $(Ca_7N_4)[In_{1.06}]$ $Ca_{obs/calcd}$ 60.5(4)/61.2 wt.%, $In_{obs/calcd}$ 26.4(2)/26.6 wt.%, $N_{obs/calcd}$ 12.5(1)/12.2 wt.%. Impurities of O, H, and C were not detected (limits of detection: $C \le 0.1$; $H \le 0.005$; $O \le 0.05$ wt%).

[23] N. F. Mott, *Philos. Mag.* **1969**, *19*, 835.

